

Central European Journal of Medicine

DOI: 10.2478/s11536-007-0040-4 Research article CEJMed 2(4) 2007 511-527

Microhardness and microstructure of deciduous enamel with different types of amelogenesis imperfecta

Alenka Pavlič^{12*}, Polona Škraba³, Ladislav Kosec⁴, Milan Petelin⁵, Satu Alaluusua⁶⁷

- Department of Pediatric and Preventive Dentistry, Faculty of Medicine, University of Ljubljana, Hrvatski trg 6, 1000 Ljubljana, Slovenia
 - ² Unit of Pediatric and Preventive Dentistry, University Medical Centre Ljubljana, 1000 Ljubljana, Slovenia
 - 3 Laboratory of Epitaxy and Nanostructures, University of Nova Gorica, 5101 Nova Gorica, Slovenia
 - ⁴ Department of Materials Science and Metallurgy, Faculty of Natural Sciences and Engineering, University of Ljubljana, 1000 Ljubljana, Slovenia
 - Department of Oral Medicine and Periodontology, Faculty of Medicine, University of Ljubljana, 1000 Ljubljana, Slovenia
 - $^{6}\ \ Department\ of\ Oral\ and\ Maxillo facial\ Diseases,\ Helsinki\ University\ Central\ Hospital,\ 00130\ Helsinki,\ Finland,$
 - Department of Pediatric and Preventive Dentistry, Institute of Dentistry, University of Helsinki, 00130 Helsinki, Finland

Received 27 June 2007; accepted 08 August 2007

Abstract: Amelogenesis imperfecta (AI) is an inherited tooth disorder with widely varying phenotypes. The aim of this study was to determine the microhardness and microstructure characteristics of the enamel in AI teeth. The AI phenotypes examined were hypoplastic (pitted and smooth form), hypomaturated, and hypocalcified. Six AI patients were diagnosed according to clinical characteristics. The microhardness of the enamel was measured on axial cuts of AI teeth acquired from the patients. The measurements were done on several sites from the enamel surface towards the dentine-enamel junction using the Vickers scale. Values of microhardness were compared to corresponding control teeth. The microstructure of AI enamel types was evaluated using scanning electron microscopy. The values of microhardness in pitted hypoplastic AI samples were, on average, lower compared to the control enamel and dropped markedly towards the dentine-enamel junction. The smooth hypoplastic enamel was not only extremely thin but also much softer than control enamel. The values for hypomaturated AI fluctuated, but the palatal sites were markedly softer than in the control tooth. Hypocalcified enamel was the softest, with values resembling those of dentin. Microstructural changes varied from altered orientation of enamel prisms in pitted hypoplastic AI to lack of normal prismatic structure and severe porosity in hypocalcified AI. The present results suggest different microhardness profiles and microstructures in each phenotype. Variations among phenotypes are expected with larger case selection in this genetically heterogeneous disease. © Versita Warsaw and Springer-Verlag Berlin Heidelberg. All rights reserved.

Keywords: Dental enamel; Amelogenesis imperfecta; Microhardness, Microstructure

^{*} E-mail: alenka.pavlic@mf.uni-lj.si

1 Introduction

The genetic disease amelogenesis imperfecta (AI) causes alteration in enamel properties and structure. By definition, deformities caused by AI are limited to defects affecting only tooth enamel. In various forms of AI, the quality and/or quantity of enamel is impaired. Due to the diversity of phenotypes, forms of inheritance (autosomal dominant, autosomal recessive, X-linked) and the lack of understanding of the causes of this disease, it is not surprising that a wide spectrum of classifications has been suggested. The first, proposed by Weinmann [1], separated the diseases into two categories only on the basis of phenotypic characteristics (inherited hypoplastic and inherited hypocalcified form of AI), and the latest, proposed by Aldred and Crawford [2], takes into consideration not only the clinical phenotype and mode of inheritance but also the genetic locus according to the type of mutation and the biochemical outcome when they are known. The classification most commonly used worldwide, which was proposed by Witkop, is based on predominant clinical manifestations and the mode of inheritance, and it distinguishes between four main types of AI. Three of the types are related to a certain stage in amelogenesis (hypoplastic, hypomaturated, and hypocalcified AI types), and the fourth is connected with taurodontism [3]. The four major forms are further subdivided into 14 subtypes; however, due to the large range of phenotypes, the classification of AI subtypes often is possible only to a limited extent, and it is important to realize that an ideal method for classifying AI has not yet been established.

Analysis shows that in the majority of enamel samples with different AI phenotypes, there are different extents of hypomineralization and hypoplasia [4–7]. According to Bäckman and Anneroth [6], in all types of AI, structural and mineral changes are present, whereas Wright and co-workers [8] reported that mineral content is reduced in hypomaturation and hypocalcified AI enamel, although in hypoplastic AI enamel, it varies from normal to reduced. Bäckman and Angmar–Mansson [5] also found that, compared to healthy enamel, especially the hypomineralized type of AI had reduced mineral content. The Witkop classification [3] uses the term hypocalcified and hypomaturation as subgroups of hypomineralized AI. Bäckman and Angmar–Mansson [5] have chosen to deviate from his terminology and categorize the hypocalcified phenotype as hypomineralized.

The microhardness of healthy enamel has been extensively reported. According to the literature, the mean microhardness value of healthy enamel for deciduous molars is 397 ± 60 Knoop hardness number (KHN) and for deciduous incisive teeth, 272 ± 26 KHN [9]. For permanent molars, two different sets of data have been presented by two different authors, namely, 343 ± 23 KHN [7] and 242 to 296 KHN [8]. Furthermore, a third author presented measurements made on axial sections (3.03 0.09 GPa) as well as on occlusal sections (3.23 ±0.28 GPa) [11]. On premolars, measurements were made on the occlusal (345 ± 5.5 KHN), midpoint (330 ± 5.9 KHN), and cervical parts (319 ± 8.7 KHN) of the enamel [10].

Microhardness varies with mineral content and prism orientation and position [13]. Specifically, the outer surface of healthy enamel shows higher values than the interior [9,

14, 15]. The rate of decrease in healthy enamel is reported to be 0.023 KHN/ μ m [10]. Variations in the results are attributed to different exposure times of enamel to fluoride and other environmental factors [16]. A positive correlation between microhardness and the mineral content in healthy enamel suggests that organic components, especially proteins and lipids, as well as inorganic components play a crucial role [17, 18]. To the best of our knowledge, there has been no previous work on microhardness of AI enamel.

The aim of this work was to determine Vickers microhardness (HV) of AI enamel from the enamel surface towards the dentine-enamel junction (DEJ) and to describe the microstructure viewed by scanning electron microscopy (SEM) in teeth representing pitted hypoplastic, smooth hypoplastic, hypomaturated, and hypocalcified types of AI.

2 Statistical methods and Experimental Procedures

2.1 Patients population

Six 5- to 16-year-old children (two female and four male) from five unrelated families with different types of AI were included in the study. Written consent from the child and the mother was obtained for participation of the study. The study was approved by the Slovenian Committee for Medical Ethics (No 24/12/04).

The patients were classified on the basis of clinical and radiographic examination (panoramic tomograms) and estimated mode of inheritance. Whenever possible, the patients were specified according to the Witkop classification [3]. To avoid exposing the patients to additional ionizing radiation, the enamel thickness was estimated from dental panoramic tomograms taken routinely during the first clinical examination of each patient suspected of having a disturbance in the development of the dentition. All patients were evaluated for unusual extra-oral findings as well as for the quality and quantity of enamel, malformed or missing teeth, and dental malocclusion. None of the patients had metabolic or endocrine defects, generalized diseases, syndromes, or fluorosis. The pedigrees of the AI families were constructed according to family history.

2.2 Tooth samples

Five deciduous teeth, two with pitted hypoplastic AI (one was type I A according to Witkop, the other was unclassified because the patient's mode of inheritance was not autosomal dominant), one with smooth hypoplastic AI (type I D), and two with hypomaturated AI (type II), one permanent tooth with hypocalcified AI (type III A), and four control teeth were examined. To avoid different levels of attrition and abrasion, which in turn could also affect the microhardness value in the experimental and control groups, all of the deciduous teeth were either extracted just before exfoliation or collected immediately after exfoliation. The third permanent molar of the 16-year-old patient with hypocalcified AI was impacted and therefore surgically removed. All teeth were stored in isotonic saline solution until microhardness tests were performed. To avoid changes

in sample structure during storage, the hardness tests were performed within days of exfoliation. The microhardness measurements were performed by a single experienced researcher (L.K.).

Each tooth was cut in half along either the bucco-palatal or bucco-lingual direction. The halves were embedded in epoxy resin with the cut side exposed. The exposed axial cross-sections were polished to 1 μ m.

2.3 Microhardness measurements

Microhardness measurements were taken on tooth cross-sections using a Vickers scale (Shimadzu, Tokyo, Japan), applying a 100-g constant load for 10 s. The first measurement was made close to the outer enamel surface. Subsequent measurements in enamel towards the DEJ junction were spaced along a line perpendicular to the enamel surface, as indicated in Fig. 1A and B. The final three measurements were performed in dentin. However, values determined in dentin were not used in any further calculations but rather served purely as a reference for quantitative comparison with the enamel measurements.

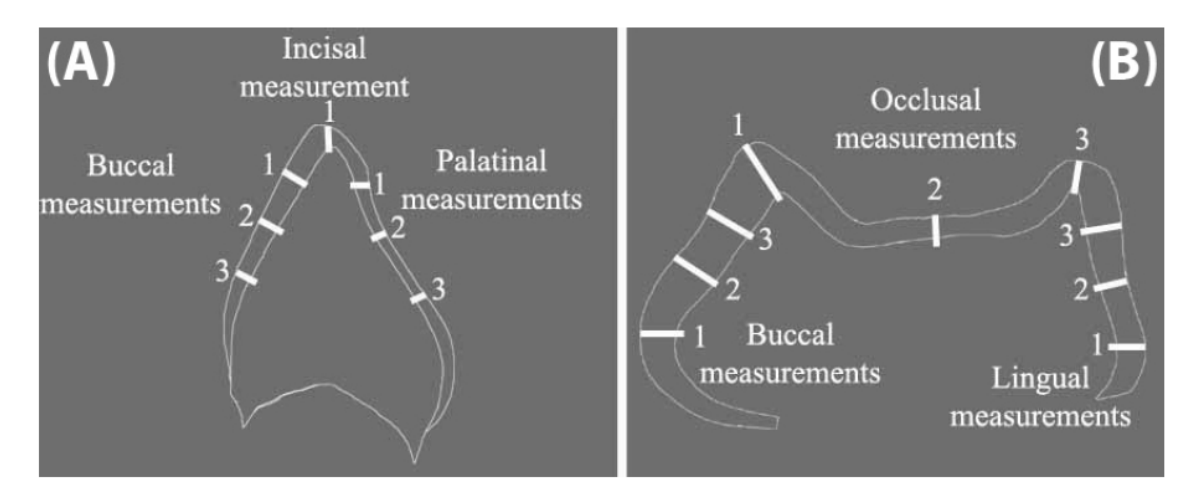


Fig. 1 Schematic illustrations of tooth cross-sections indicate the lines along which microhardness measurements were taken. For each sample, measurements were made along three buccal and three palatal/lingual lines, with additional measurements made along (A) one incisal line in incisive and canine teeth or (B) three occlusal lines in molars. The first measurement was made close to the outer enamel surface and subsequent measurements were made along the direction toward the DEJ.

As indicated in Fig. 1A and B, measurements were made along three buccal and three palatal/lingual lines for each sample. Depending on the tooth type, measurements were also made either along three occlusal lines or one incisal line. The resulting values along all lines for either selected surface were plotted with microhardness as a function of the distance of the measurement from the outer enamel surface. If the tooth, through attrition, no longer had an incisal edge, the measurements could not be made and therefore do not appear in the graph (Fig. 2). In each sample, the distances between measurements

were adjusted according to the variation in hardness and the zone of influence from one measurement to another. The distance between individual measurements was equal to the length of the region affected by the measurement (zone of influence), thereby ensuring that one measurement did not influence the subsequent measurement. Distances between adjacent measurements in each sample line were equidistant and distributed evenly in the control teeth. The measurements were taken in relation to either the enamel surface or the DEJ, or, in the case of pitted hypoplastic enamel, in relation to the pits. This assured that surface characteristics would not influence the results.

A control group of four clinically healthy teeth were tested in a similar way as the AI teeth. Because no control teeth from unaffected family members were available, healthy teeth were obtained from unrelated patients. The teeth consisted of four different tooth types, deciduous incisive, deciduous canine, deciduous molar, and permanent molar, each of which corresponded to the tooth type of the AI samples. The test/control tooth pairs were thus 74/64, 55/64, 82/72, 53/53, 53/53, and 28/28. The total number of measurements for each surface ranged from 5 to 62 for the AI teeth and from 6 to 51 for the control teeth (Table 1). The microhardness measurements made on all of the healthy control teeth displayed a best fit to a logarithmic curve. Despite the variations observed in microhardness measurements made on the different AI enamel, all samples were fitted to logarithmic curves to obtain consistent and comparable results.

2.4 Scanning electron microscopy

The microstructure of AI enamel was observed using SEM. After microhardness measurements were completed, the samples were polished, dehydrated with 70% alcohol, dried, sputter-coated with a thin carbon layer in a vacuum (Vacuum Evaporator, Type JEE-SS; JEOL, Tokyo, Japan) and examined by SEM (JEOL JSM - 5610; JEOL). To observe the microstructure more clearly, all the samples, except the tooth with hypocalcified AI, were subsequently repolished and etched with 37% H₃PO₄ for 30 s and then rinsed with a distilled water spray for 30 s, dried with compressed air, dehydrated with 70% alcohol, dried again, and sputter-coated with carbon (Vacuum Evaporator, Type JEE-SS; Japan Electron Optics, Tokyo, Japan). Once again, the samples' etched enamel was examined by SEM. Images were obtained at magnifications between 110× and 1200×.

2.5 Statistical analysis

Differences in microhardness values between the surfaces of each AI tooth and that of the healthy control tooth were compared by covariance analysis using the distance from the enamel surface as a covariate. Differences between different control tooth types were also compared. Differences between the pitted hypoplastic samples as well as differences between each of pitted hypoplastic samples and the corresponding control tooth were compared using the t-test for differences in the slopes of regression lines.

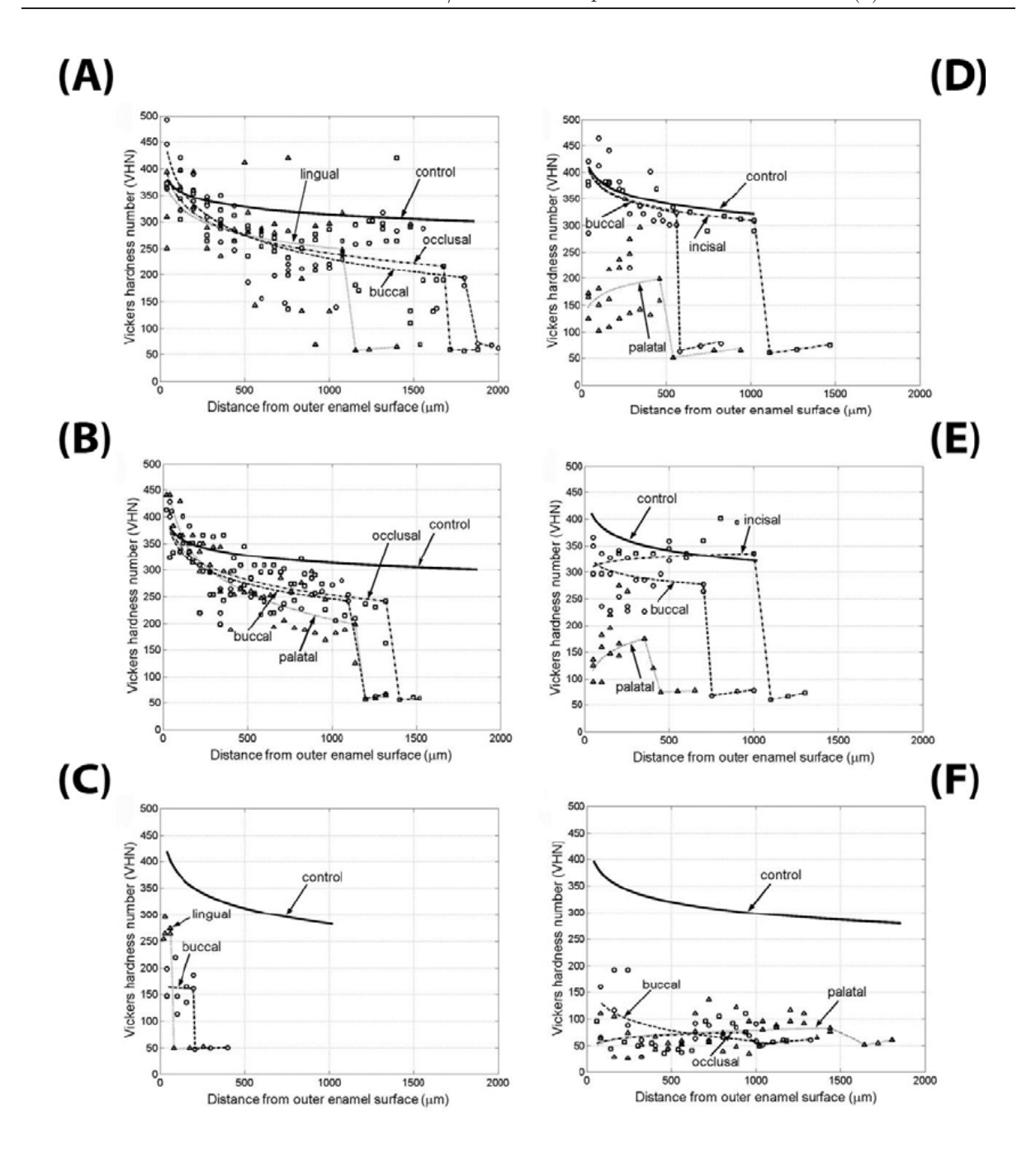


Fig.2 Microhardness values and profiles of each AI sample are presented on individual graphs. The individual microhardness measurements are represented as triangles for the palatal/lingual surface, circles for the buccal surface, and squares for the incisal/occlusal surface. Each graph contains three logarithmic curves representing measurements on the three different AI tooth surfaces: palatal/lingual (••••), buccal (---), and incisal/occlusal (-•-). The length of this curve also represents the thickness of the enamel on that particular surface. A sudden drop in values, represented by an almost vertical line, indicates the DEJ, whereas the last three values, fitted to a line, represent measurements made in dentin. For comparative purposes, the fitted logarithmic curve of microhardness measurements of the corresponding healthy control tooth, taken from multiple measurements of the palatal/lingual, buccal, and incisal/occlusal surfaces, is drawn as a solid line. (A, B)

Microhardness of enamel in both pitted hypoplastic AI teeth, first left deciduous mandible molar, and second right deciduous maxillary molar, were comparable to healthy enamel at the enamel surface but decreased markedly as the measurements moved further into the bulk of enamel. (C) Microhardness of enamel with smooth hypoplastic AI of second right deciduous mandible incisor revealed very low microhardness values compared to a healthy control tooth. (D, E) Both samples with hypomatured type of AI were right deciduous maxillar canines for patients A and B respectively. There was a distinct difference in the microhardness profile between various surfaces when compared to a healthy control tooth. Both samples displayed fluctuations of the microhardness values from the outer surface toward the DEJ. (F) The microhardness of enamel of the third left permanent maxillary molar with hypocalcified AI was very low for each examined surface site and far lower than those measured in the healthy control tooth.

3 Results

3.1 Family pedigrees and phenotypes

The 9-year-old girl from family 1 had pitted hypoplastic AI. Because no other family member was known to have similarly altered enamel, the case was likely to be either sporadic or due to an autosomal recessive mode of inheritance. The thickness of enamel was normal, otherwise hard and whitish, with small pinpoint sized pits on its surface. Some of the pits were darkly colored. Contrast between dentin and enamel on the dental panoramic tomograms could be distinguished.

Dental examination of the 11-year-old girl from family 2 also indicated pitted hypoplastic AI. Family history revealed that the proband's mother, the mother's two brothers, the grandfather and his sister, and the great-grandmother had similarly altered enamel. The estimated mode of inheritance was autosomal dominant. The color of the enamel was generally whitish, with some parts yellowish. The enamel surface was hard and covered with small pits (Fig. 2A). The most distinct changes were in the cervical part of teeth. Dental panoramic tomogram confirmed normal thickness of enamel and contrast between dentin and enamel (Fig. 2B).

The 9-year-old boy from family 3 had smooth hypoplastic AI. The patient's brother and father had similarly altered dentition. The mode of inheritance was autosomal dominant. The color of permanent teeth was yellow-brown, and the deciduous teeth were yellowish (Fig. 2C). All teeth had extensive attrition occlusally. Orthodontic assessment estimated molar relations mandible protrusion in the saggital plane (Angle class III occlusion) with left and right crossbites in the horizontal plane. Right deciduous canine and incisors were also in crossbite. The enamel was so thin that the crowns could barely be seen on the dental panoramic tomogram enamel outlining (Fig. 2D).

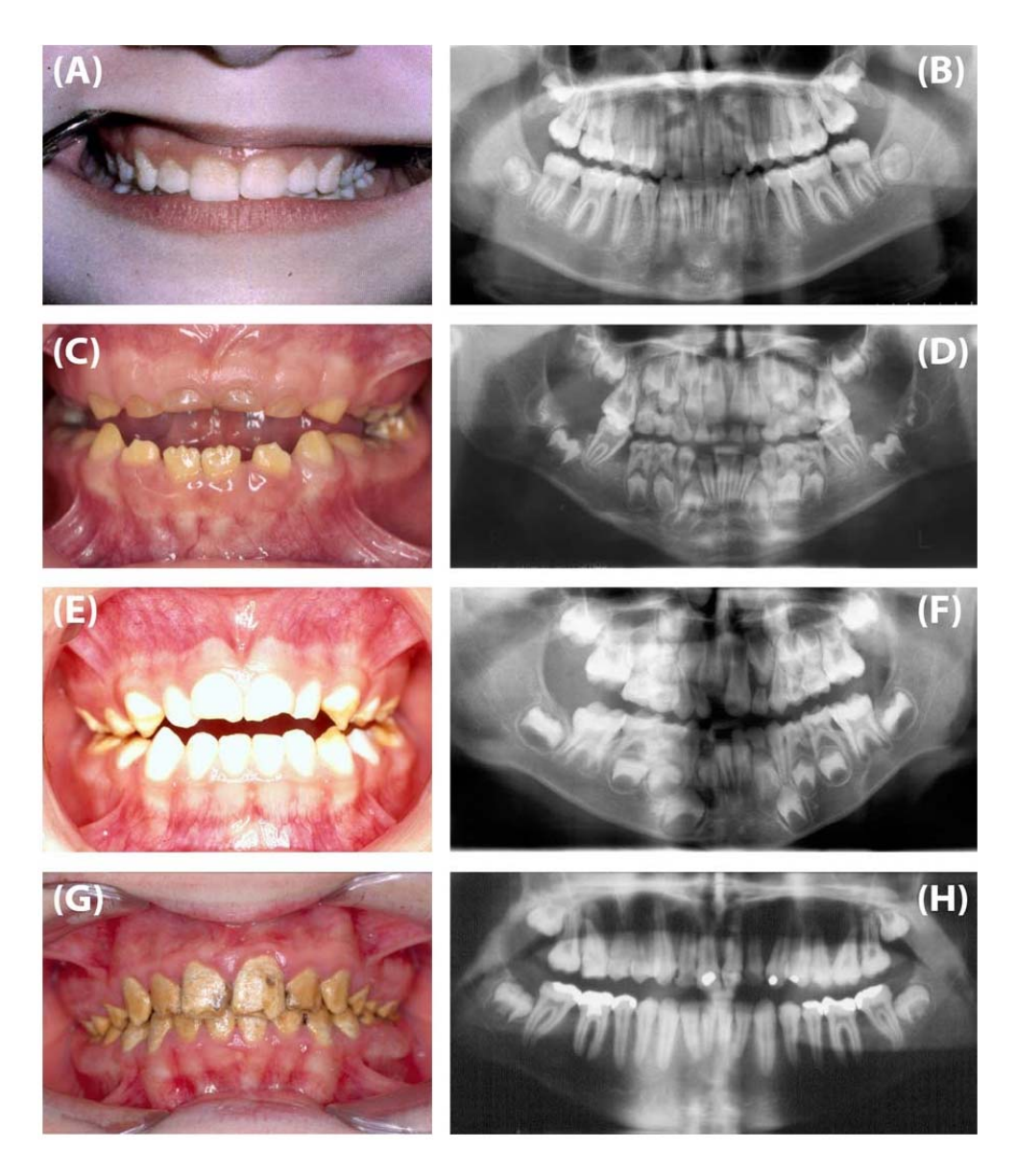


Fig.3 (A) Clinical appearance and (B) the dental panoramic tomogram of the 11-year-old girl were consistent with a diagnosis of pitted hypoplastic AI. The enamel surface was hard and covered with small, pinpoint- to pinhead-sized pits. (C) Phenotype and (D) the dental panoramic tomogram of the 9-year-old boy with smooth hypoplastic AI revealed severe alteration in the quality and especially in the quantity of enamel. (E) Clinical appearance and (F) the dental panoramic tomogram of the 5-year-old boy with hypomaturated AI revealed enamel of original normal thickness but altered quality. (G) Clinical appearance and (H) the dental panoramic tomogram of the 16-year-old boy with hypocalcified-type AI revealed a profoundly altered enamel quality.

Table 1 Results of various techniques used for the detection of Parvovirus B19 induced fetal hydrops and distribution of sections evaluated in the study.

	Sample tooth type	Buccal Mean values \pm SD a (HV)	b	Incisal/occlusal Mean values $_{\rm m}$ \pm SD a (HV)		Palatal/lingual Mean values $_{\rm I}$ \pm SD a (HV)	nal n	Overall average Mean values $n \pm SD^a$ (HV)	$\underset{\mathbf{n}}{\operatorname{age}}_{b}$
AI	74 (pitted hypoplastic)	281.0 ± 85.0	39	263.9 ± 69.1	62	288.1 ± 82.7	33	274.9 ± 77.5	134
engmer	55 (pitted hypoplastic)	288.1 ± 52.5	41	288.7 ± 55.1	54	284.3 ± 79.3	43	287.2 ± 62.5	138
	82 (smooth hypoplastic)	162.0 ± 33.9	6	¢-	<i>٠</i>	270.0 ± 15.9	ಬ	200.7 ± 60.8	14
	53 (hypomaturation-A c)	367.1 ± 48.2	20	341.3 ± 32.4	10	165.7 ± 49.0	16	291.5 ± 103.5	46
	53 (hypomaturation-B c)	301.6 ± 41.5	14	342.7 ± 34.9	10	160.3 ± 52.3	12	265.9 ± 88.2	36
	28 (hypocalcified)	72.6 ± 26.7	52	73.5 ± 24.7	37	79.4 ± 36.8	38	74.9 ± 29.5	127
Control enamel	64 (control)	332.8 ± 48.3	38	362.4 ± 42.1	16	355.5 ± 42.5	30	346.5 ± 46.2	84
	72 (control)	367.6 ± 56.2	11	387.1 ± 53.2	-	360.3 ± 52.0	13	364.6 ± 57.8	31
	53 (control)	375.7 ± 18.2	9	375.3 ± 34.3	1 -	369.3 ± 34.9	17	378.7 ± 31.0	30
	28 (control)	345.6 ± 46.0	25	311.5 ± 41.1	51	333.9 ± 45.5	34	326.2 ± 45.5	110

 a Mean values (± SD) by HV) are given for each individual surface of the tooth. b Number of measurements for each individual surface of the tooth.

Two boys from family 4 presented hypomaturated type of AI. The older, 10-yearold boy, had mixed dentition with hypomaturated, yellowish, and slightly softer enamel. Along with poor dental aesthetics, he complained of tooth hypersensitivity. The enamel thickness was normal but it chipped away easily. In permanent dentition the enamel was altered on all surfaces. In the deciduous teeth, the enamel on the buccal and oral surfaces of the molars and the buccal surface of the incisors and canines was in better condition.

The 5 year-old younger brother from family 4 with hypomaturated AI also had an anterior open bite. The enamel was chalky-like whitish with chipping of incisal or occlusal parts of the tooth crown, exposing underlying yellowish enamel and dentin (Fig. 2E). On the dental panoramic tomogram, the thickness of the enamel, where it was not chipped away, was normal, but the differences in radiodensity of dentin and enamel were difficult to distinguish (Fig. 2F). The boys' father had similarly altered enamel. Parentage of the grandfather or his ancestors on the father's side was not known. The mother and all of her relatives had normal enamel. The pedigree was consistent with an autosomal dominant mode of inheritance.

The enamel of the 16-year-old boy in family 5 was hypocalcified, soft, and dark yellow-brownish upon eruption. The pedigree suggested autosomal dominant inheritance. Dental aesthetics of the boy's teeth were extremely poor (Fig. 2G). The surface was rough. Soft and dark yellow-brownish enamel upon eruption of his complete permanent dentition was chipping away, exposing large areas of dentin. Mostly, enamel was chipped away on incisal and occlusal parts of the tooth. On the dental panoramic tomograms, no contrast between dentin and enamel could be observed (Fig. 2H).

3.2 Microhardness

The mean microhardness values of the control teeth varied from 326 ± 45.5 to 379 ± 31.0 HV. The outer surface of healthy enamel showed higher values than the interior. Covariance analysis of microhardness between different surfaces of individual control teeth showed no statistically significant differences (p > 0.05). However, the analysis of microhardness between different control tooth types did result in a significant difference (p < 0.001). Therefore, comparison of microhardness of each AI tooth to the corresponding control tooth type was justified.

In general, AI teeth had lower microhardness values than the control teeth (Table 1, Fig. 2). Microhardness profiles in both pitted hypoplastic AI teeth (one was of type I A and the other was unclassified) were very similar (Fig. 2A and B). The values as measured for the three surfaces and for both teeth at the outer surface showed even higher numbers than the control enamel (380 HV), but decreased going further into the bulk, finally reaching values approximately 50 HV lower than control enamel at the DEJ (280 HV). Logarithmic curve slope analysis showed that the values were lower than those of the control tooth (p < 0.001; Fig. 2A and B).

The tooth sample clinically determined as having smooth hypoplastic AI (type I D) had extremely thin enamel. The thickest enamel was on the buccal surface, measuring

 $230~\mu\text{m}$, while the thin enamel on the lingual surface measured only $90~\mu\text{m}$. Along with the extremely thin enamel observed in this tooth, very low microhardness values (average 201~HV) compared to the control tooth were measured. The few measurements obtained showed mean values that were approximately 160~HV lower than those measured on the control tooth (Fig. 2C). On average, the lowest values were obtained from the buccal sites.

The microhardness profiles of the examined hypomaturation AI teeth had many common features (Fig. 2D and E). Enamel on both teeth with hypomaturated AI was of normal thickness, but microhardness values showed a distinct difference between the buccal and incisal sites and the palatal sites. The palatal sites were softer than the other two surfaces, with values around 150 HV at the outer surface, increasing toward the DEJ (Fig. 2D and E). The shape of the logarithmic slope of the buccal site values and of the incisal site of one sample followed that of the control slope, whereas more fluctuation was seen in the incisal sites of the other sample.

In the hypocalcified enamel sample (type III A), the microhardness was very low on each examined surface site(s) (Table 1). Average values of approximately 75 HV were comparable to those found in dentin (Fig. 2F). The lowest values were measured in the region 300 to 600 μ m from the surface.

3.3 Scanning electron microscopy

The enamel microstructure in all AI types was altered to varying extents. The least alteration was observed for the pitted hypoplastic AI samples. Both pitted hypoplastic AI samples (type I A sample and the unclassified sample) revealed thickness of enamel comparable to thickness of normal enamel. Enamel prisms of twisted courses were present throughout the bulk of the enamel. Pits were scattered on the enamel surface (Fig. 2A). Otherwise, a normal aprismatic layer was lining the enamel surface.

In the smooth hypoplastic AI sample (type I D), an extraordinarily thin layer of enamel covered the dentin. Enamel was insufficient in quantity as well as in quality (Fig. 2B). Throughout the enamel thickness, the microstructure was deficient, with poorly formed and inadequately mineralized prisms. Empty spaces, the size of prisms, were also present on different locations throughout the bulk of the enamel. At the surface, there was no aprismatic enamel.

Enamel with hypomaturated AI (type II) revealed irregularly distributed regions with well-defined normal prisms, with either etched prism heads or sheath spaces and regions with poorly defined or even unrecognizable enamel structure (Fig. 2C). In places where sheath spaces were widened, prisms were of uneven size and showed different levels of porosity.

The enamel of the hypocalcified AI tooth (type III A) revealed a markedly altered microstructure. Poorly mineralized enamel lacked a normal prismatic structure throughout the thickness of the enamel (Fig. 2D). The enamel showed severe porosity, and in some locations, empty spaces fused into branching defects. Furthermore, in the hypocalcified

AI sample, pits similar to those found on the pitted hypoplastic AI sample were observed on the rough surface (Fig. 2E).

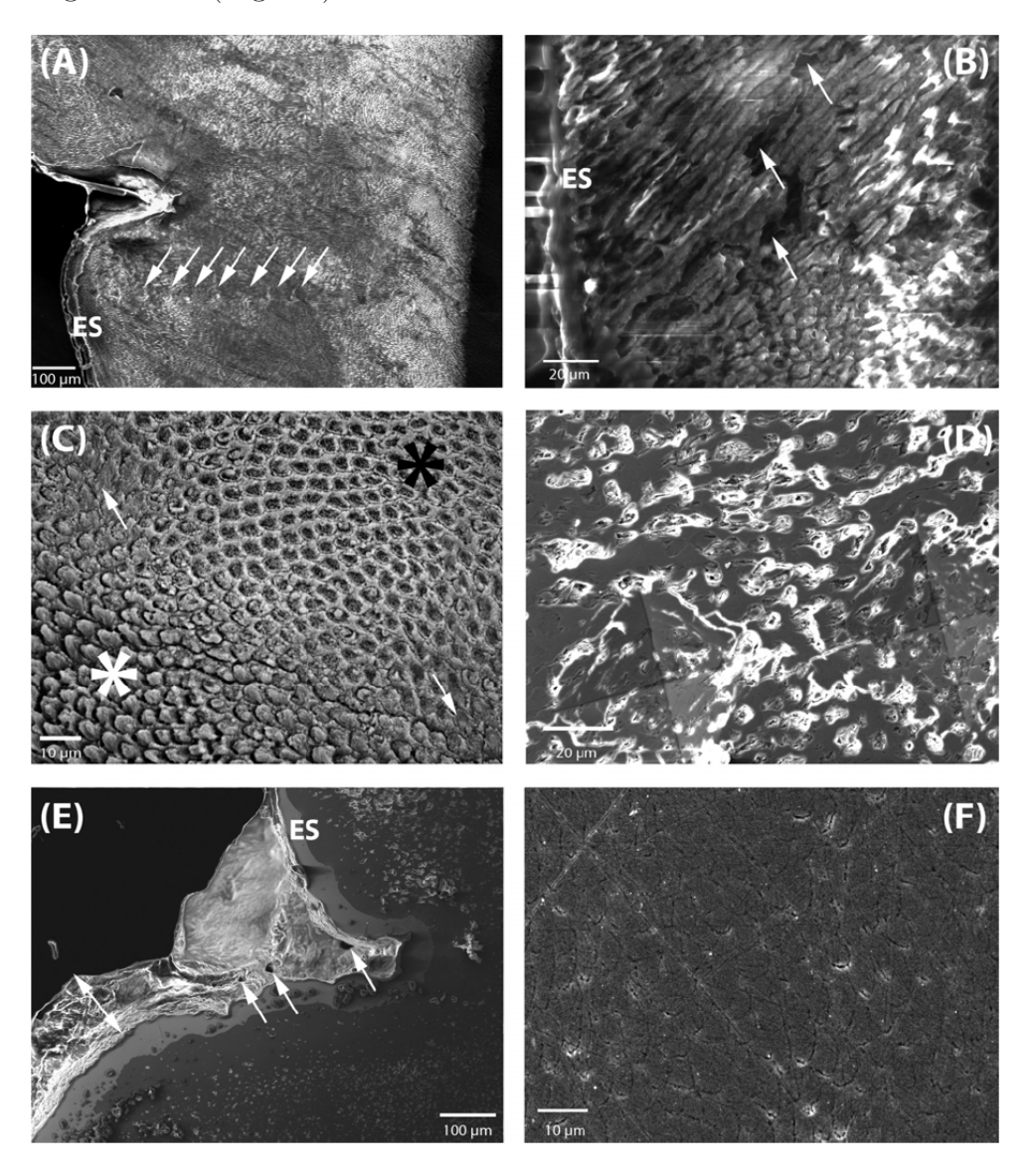


Fig.4 Enamel microstructure of AI samples, on which microhardness was measured, was viewed by SEM. (A) Pitted hypoplastic AI enamel (second right deciduous maxillary molar) was of normal thickness with twisted prisms course in the bulk of enamel. An obvious pit is present on the enamel surface. Indentations of microhardness measurements (underlined) can be seen (etched, $110\times$). (B) Smooth hypoplastic AI enamel (second right deciduous mandible incisor) was not only exceptionally thin but also of poor microstructure. Between deficiently formed and inadequately mineralized prisms, empty spaces the size of prisms were present, some of which are marked with arrows (etched, $650\times$). (C) Hypomaturated AI (right deciduous maxillary canine; tooth 53-B in Table 1) revealed areas with etched prism heads and less-etched preserved sheath spaces (black asterisk). In other areas, the situation was reversed, with prism heads being preserved (white asterisk). There were some areas where the prism structure was poorly defined or even unrecognizable (arrows) (etched, $1000\times$). (D) Two indentations of microhardness

measurements are visible in the bulk of severely porous hypocalcified AI enamel (the third left permanent maxillary molar; tooth 28) (unetched, $700\times$). (E) On the enamel surface of hypocalcified AI enamel, pits were observed. Note the small orifices (arrows) opening to the pit and the rough surface (arrow) of the enamel (unetched, $130\times$). The microstructure of hypocalcified type of AI revealed the most poorly mineralized enamel as compared to enamel of other AI samples and especially to (F) the enamel of healthy control teeth. Unetched healthy enamel (a second left deciduous mandible molar) displayed well-mineralized enamel prisms through the entire thickness of the enamel. Due to the high quality of mineralization and very narrow sheath space, individual prisms were barely distinguishable (unetched, $1200\times$). ES, enamel surface. Scale bars (in microns) are shown for each of the panels.

4 Discussion

In the present study, we examined teeth that, on the basis of their phenotype, represented hypoplastic, hypomaturated and hypocalcified types of AI. The results suggested that, in general, the microhardness of AI enamel was lower than that of the control enamel and that a characteristic microhardness profile was indicated for each phenotype. In pitted hypoplastic AI samples, the microhardness values dropped markedly from the enamel surface towards the DEJ. The smooth hypoplastic enamel was not only extremely thin but also much softer than control enamel. The values for hypomaturated AI fluctuated from the enamel surface towards the DEJ and on different sites of the tooth. Hypocalcified enamel was the softest, with values resembling those of dentin, throughout the enamel.

Enamel with pitted hypoplastic AI had, regardless to the mode of inheritance, normal enamel thickness with pits on the surface, which is in accordance with the description of clinical characteristics of type I A according to Witkop [3]. The microstructure of pitted hypoplastic AI enamel revealed pits on the surface and well-defined prisms throughout the enamel. However, the main changes in microhardness were not found to be on the superficial layer of enamel, as implied by Witkop's clinical description [3], but rather in layers within the bulk of the enamel. It seems likely that mineralization of the bulk of AI enamel is insufficient compared to normal enamel during teeth eruption into the oral cavity. Wright and coworkers [19] described a similar trend of Ca values in hypoplastic enamel. They stated that as one moves towards the DEJ, the Ca content falls more drastically than in healthy teeth, with the layer 30 μ m from the junction having an extremely low Ca content. Contrary to our microhardness observations, Bäckman and Angmar-Mansson reported that the mineral distribution pattern, as assessed by qualitative microradiography, from the enamel surface to DEJ was similar in pitted hypoplastic AI and normal teeth [5]. However, the range for the mineral content per volume was similar to normal in only one of the four pitted hypoplastic AI teeth analyzed [5].

The enamel of smooth hypoplastic AI was not only very thin in the buccal and lingual surfaces but also of poor quality. Due to attrition, no enamel was present in the incisal surface. Extensive reduction in the width as well as poor mineralization was observed by

SEM. The enamel microstructure revealed deficiently formed enamel prisms with widened interprism spaces and microhardness values that were, on average, 200 HV lower compared to normal enamel. The finding of low microhardness values is in agreement with previous reports and with our SEM observations. Specifically, it has been reported that smooth hypoplastic enamel is not only very thin but also generally porous, lacking normal prismatic structure in certain areas [19]. Furthermore, this type of enamel surface has been described as containing demineralized pores or openings 5 to 20 μ m in diameter, which, on an axial cut, appear as demineralized canals running perpendicularly from the surface [4]. Based on the quality changes of microstructure and microhardness in smooth hypoplastic AI, which is designated as type I D in Witkop's classification, these samples could be also classified as showing hypomineralized of AI.

In both samples with hypomatured AI, the microhardness values fluctuated from the outer surface toward the DEJ, and there was a distinct difference in the microhardness profile between various surfaces. Uneven microhardness values correlated with uneven microstructures, represented by different sizes of enamel prisms and interprism spaces. This revealed unevenly dispersed areas with sufficiently formed enamel prisms, poorly formed prisms, and even areas of unrecognizable microstructure. According to Shore and coworkers, in hypomaturated AI with different inheritance patterns (autosomal dominant, autosomal recessive, sporadic, and X-linked) the structure and elemental composition show are similar between the samples [20]. SEM analysis revealed regions where prisms and constituent crystals appeared to be largely obscured by amorphous material, and microradiography indicated a reduced radiodensity. In the affected areas, the carbon content was increased up to fivefold. Outside these areas, the enamel composition was indistinguishable from control teeth [20]. The authors conclude that the phenotype classified clinically as hypomaturated AI is indeed associated with consistent structural and compositional defects, regardless of the mode of inheritance. It is possible that the unique structure described by Shore and coworkers could partly explain the wide distribution of microhardness values in our hypomaturation AI samples.

Reports on the various forms of AI indicate that the hypocalcified type of enamel has a low volume percentage of minerals and that the lowest values are found in the bulk of the enamel [5]. As much as a 30% decrease in mineral content has been reported in this type of enamel [21]. In line with clinical and microstructural findings related to hypocalcified AI, our results indicated very low and consistent microhardness values at all surface sites. Although not etched, the hypocalcified AI enamel sample observed by SEM was extremely porous. On the rough enamel, surface pits were observed, similar to those found on pitted hypoplastic AI enamel.

Both the hypocalcified AI tooth and the control tooth were maxillary wisdom teeth. The AI tooth was obtained from a 16-year-old patient. The crown and approximately half of the root were formed, and the furcation zone was fully developed. Because root formation typically starts after the enamel is nearly completely mineralized, with the exception of post-eruptive mineralization, it is likely that enamel mineralization of tooth 28 was almost completed. Thus, it could be comparable to a fully developed tooth. Fur-

thermore, during amelogenesis, normal mineralization is not completed simultaneously in different parts of the enamel, and the cervical region is the last to mineralize completely. Despite the fact that the hypocalcified AI tooth (28) had a much lower overall microhardness, no significant differences in microhardness values were found between the cervical region and other parts of the enamel. This suggests that at this stage of development, mineralization of the enamel was already completed.

Microhardness measurements indicate a material's relative resistance to wear, that is, harder materials are more likely to wear at a slower rate. The hardness of healthy enamel stems from its prismatic structure and its organic and inorganic content. Lower microhardness in AI-diagnosed enamel, in general, shows that this enamel is structurally different from healthy enamel and has a lower content of minerals and a higher content proteins and lipids. Indeed, teeth diagnosed with different types of AI have an altered structure [6, 8, 17, 20] and impaired mineralization [5, 6, 17, 20]. In hypomineralized areas of enamel in different AI types, the amount of Ca has been found to be lower than in normally mineralized areas [8]. Quality as well as quantity of minerals has also been found to be altered in AI enamel [5, 6]. Also, analysis of the amount and size of protein molecules and their amino acid composition in various types of AI shows differences from healthy enamel [23, 24]. How various minerals, proteins and, lipids affect the microhardness requires further investigation.

The present results suggest that characteristic microhardness profiles and microstructures in each phenotype be analyzed. Although the microstructure in pitted hypoplastic AI samples seemed normal, the microhardness values were lower than in the control enamel and dropped markedly towards the DEJ. Obviously, the quality of the bulk of the pitted hypoplastic AI enamel was altered. The high values of microhardness in the superficial layer of pitted hypoplastic AI samples are the values in healthy enamel, which might be due to an undisturbed process of continuing enamel mineralization after tooth eruption. Furthermore, the smooth hypoplastic AI enamel was altered in quantity as well as in quality. Comparison between hypomaturated and hypocalcified AI enamel reveals that in hypomaturated enamel, microhardness values fluctuated, and the microstructure was uneven. Severely porous hypocalcified enamel, on the other hand, completely lacked a normal prismatic structure, with very low but uniform values of microhardness. Variations among phenotypes are expected to be found with larger case selection in this genetically heterogeneous disease.

In conclusion, microhardness measurements on cross-sections combined with microstructural studies allowed us to analyze enamel from various phenotypes of AI, from different surfaces of the AI teeth, and at different depths of enamel. The present results from a limited number of teeth examined suggest that each phenotype has a characteristic microstructure and microhardness profile when measured from the outer enamel towards the DEJ. Each profile differs markedly from that of healthy enamel, with the majority of microhardness values being lower than those of the control enamel. Further studies will relate the present mechanical and microstructural findings with gene defects causing AI in each patient.

Acknowledgements

The authors would like to thank Professor Andrej Blejec from the Slovenian National Institute of Biology for providing the statistical analysis of our results and Ms. Nika Breskvar for expert technical assistance.

References

- [1] J.P. Wainmann, J.F. Svoboda and R.W. Woods: "Hereditary disturbances of enamel formation and calcification", *J. Am. Dent. Assoc.*, Vol. 32, (1945), pp. 397–418.
- [2] M.J. Aldred and P.J.M. Crawford: "Amelogenesis imperfecta-towards a new classification", *Oral Dis.*, Vol. 1, (1995), pp. 2–5.
- [3] C.J. Witkop: "Amelogenesis imperfecta, dentinogenesis imperfecta and dentin dysplasia revisited: problems in classification", *J. Oral. Pathol.*, Vol. 17, (1989), pp. 547–553.
- [4] B. Bäckman, G. Anneroth and P. Hörstedt: "Amelogenesis imperfecta: a scanning electron microscopic and microradiographic study", *Oral. Pathol.*, Vol. 18, (1989), pp. 140–145.
- [5] B. Bäckman and B. Angmar–Mansson: "Mineral distribution in the enamel of teeth with amelogenesis imperfect as determined by quantitative microradiography", Scan. J. Dent. Res., Vol. 102, (1994), pp. 193–197.
- [6] B. Bäckman and G. Anneroth: "Microradiographic study of amelogenesis imperfecta", Scan. J. Dent. Res., Vol. 97, (1989), pp. 316–329.
- [7] B. Bäckman, T. Lundgren, U. Engström, L.K.L. Falk, J.M. Chabala, R. Levi–Setti and J.G. Norén: "The absence of correlations between a clinical classification and ultrastructural findings in amelogenesis imperfecta", *Acta Odontol. Scand.*, Vol. 51, (1993), pp. 79–89.
- [8] J.T. Wright, T.G. Deaton, K.I. Hall and M. Yamauchi: "The mineral and protein content of enamel in amelogenesis imperfecta", Connect. Tissue Res., Vol. 32, (1995), pp. 247–252.
- [9] R.G. Craig and F.A. Peyton: "The microhardness of enamel and dentin", *J. Dent. Res.*, Vol. 37, (1958) pp. 661–668.
- [10] N. Meredith, M. Sherriff, D.J. Setchell and S.A.V. Swanson: "Measurement of the microhardness and Young's modulus of human enamel and dentine using an indentation technique", *Arch. Oral. Biol.*, Vol. 41, (1996), pp. 539–545.
- [11] H.H. Xu, D.T. Smith, S. Jahanmir, E. Romberg, J.R. Kelly, V.P. Thompson and E.D. Rekow: "Indentation damage and mechanical properties of human enamel and dentin", J. Dent. Res., Vol. 77, (1998), pp. 472–480.
- [12] D. Purdell–Lewis, A. Groeneveld and J. Arends: "Hardness tests on sound enamel and artificially demineralized white spot lesions", *Caries Res.*, Vol. 10, (1976), pp. 201–205.
- [13] J.L. Cuy, A.B. Mann, K.J. Livi, M.F. Teaford and T.P. Weihs: "Nanoindentation

- mapping of the mechanical properties of human molar tooth enamel", Arch. Oral. Biol., Vol. 47, (2002), pp. 281–291.
- [14] H.F. Atkinson and P. Saunsbury: "An investigation into the hardness of human enamel", Br. Dent. J., Vol. 94, (1953), pp. 250–253.
- [15] K. Fokuda, S. Higashi, K. Miake and T. Matsui: "Studies on microhardness of the human third molar, especially that of the enamel", *Bull. Tokyo. Dent. Coll.*, Vol. 16, (1975), pp. 11–33.
- [16] E. Mahoney, A. Holt, M. Swain and N. Kilpatrick: "The hardness and modulus of elasticity of primary molar teeth: an ultra-micro-indentation study", J. Dent., Vol. 28, (2000), pp. 589–594.
- [17] J.D.B. Featherstone, J.M. ten Cate, M. Shariati and J. Arends: "Comparison of artificial caries-like lesions by quantitative microradiography and microhardness profiles", *Caries. Res.*, Vol. 17, (1983), pp. 385–391.
- [18] T. Kodaka, K. Debari, M. Yamada and M. Kuroiwa: "Correlation between microhardness and mineral content in sound human enamel", Caries. Res., Vol. 26, (1992), pp. 139–141.
- [19] J.T. Wright, C. Robinson and R. Shore: "Characterization of the enamel ultrastructure and mineral content in hypoplastic amelogenesis imperfecta", *Oral. Surg. Oral. Med. Oral. Pathol.*, Vol. 72, (1991), pp. 594–601.
- [20] R.C. Shore, B. Bäckman, S.J. Brookes, J. Kirkham, S.R. Wood and C. Robinson: "Inheritance pattern and elemental composition of enamel affected by hypomaturation amelogenesis imperfecta", *Connect. Tissue. Res.*, Vol. 43, (2002), pp. 466–471.
- [21] J.T. Wright, M.J. Aldred, P.J.M. Crawford, J. Kirkham and C. Robinson: "Enamel ultrastructure and protein content in X-linked amelogenesis imperfecta", *Oral. Surg. Oral. Med. Oral. Pathol.*, Vol. 76, (1993), pp. 192–199.
- [22] M.J. Aldred, P.J.M. Crawford, W. Rowe and R.P. Shellis: "Scanning electron microscopic study of primary teeth in X-linked amelogenesis imperfecta", J. Oral. Pathol. Med., Vol. 21, (1992), pp. 186–192.
- [23] J.T. Wright and W.T. Butler: "Alteration of enamel proteins in hypomaturation amelogenesis imperfecta", J. Dent. Res., Vol. 86, (1989), pp. 1328–1330.
- [24] Y. Takagi, H. Fujita, H. Katano, H. Shimokawa and T. Kuroda: "Immunochemical and biochemical characteristics of enamel proteins in hypocalcified amelogenesis imperfecta", Oral. Surg. Oral. Med. Oral. Pathol. Oral. Radiol. Endodont., Vol. 85, (1998), pp. 424–430.